

DIAGNOSTICS AND CONTROL OF WAVENUMBER STABILITY  
AND PURITY OF TUNABLE DIODE LASERS RELEVANT TO  
THEIR USE AS LOCAL OSCILLATORS IN HETERODYNE SYSTEMS\*

S. Poultney, D. Chen, G. Steinberg, F. Wu, A. Pires, M. Miller,  
and M. McNally  
The Perkin-Elmer Corporation, Norwalk, CT. 06856

SUMMARY

Performance characteristics inherent to both available tunable diode lasers and their environment will affect their use as local oscillators in heterodyne systems. This paper reports diagnostics of wavenumber stability and purity of tunable diode lasers in closed cycle cooler environments, and a new concept for control of the wavenumber in heterodyne system applications. The inherent TDL characteristics included the capability to be tuned to the wavenumber desired, the change in operating point as a function of time and thermal cycling, the nonlinear dependence of wavenumber on drive current, the axial mode structure, and the observed fine structure of "single" axial modes.

Initial operation of the TDL showed that it was not possible to adjust the wavenumber to one selected a priori in the TDL tuning range. Its operating point was recorded as a function of time and thermal cycling by heterodyne and absorption techniques. During operation, the operating point would change by  $0.1 \text{ cm}^{-1}$  over the longer term with even larger changes occurring during some thermal cycles. Most changes during thermal cycling required using lower temperatures and higher currents to reach the former wavenumber (when it could be reached). In many cases, an operating point could be selected by changing TDL current and temperature to give both the desired wavenumber and most of the power in a single mode. The selection procedure had to be used after each thermal cycling. Wavenumber nonlinearities of about 10% over a 0.5-cm tuning range were observed. Diagnostics of the single mode selected by a grating monochromator showed wavenumber fine structure under certain operating conditions. The characteristics due to the TDL environment included short-term wavenumber stability, the instrument lineshape function, and intermediate-term wavenumber

---

\* This work was partially supported by the High Altitude Pollution Program, Contract No. FAA-AEE-79. However, the primary sources of support were Perkin-Elmer's Independent Research and Development Programs and capital expenditures. S. Poultney wishes to thank Dr. David A. Huchital, Director of Research, for hosting the measurement programs and for having the foresight to provide the initial capital support.

stability. Steinberg (ref. 1) has reported wavenumber set-point stabilities of several MHz on the short term (up to several minutes). His heterodyne measurement of this stability indicated that the instrumental line-shape function had a half-width of 10 MHz and a shape with broad wings and that the wings were due to residual cooler vibrations which could not be removed. Preliminary work with digital control of TDL current indicates an intermediate-term wavenumber stability (up to an hour) of  $10^{-3} \text{ cm}^{-1}$  or better which is related to cycling of the temperature control system.

These wavenumber stability and purity characteristics will require supplementary systems to ensure that the TDL will be an appropriate local oscillator, especially if thermal cycling may occur. We have developed the following concept for wavenumber control such that the TDL wavenumber can be adjusted to and held at the desired wavenumber location in the absence of a calibration cell containing the gas to be measured. The wavenumber control algorithm is designed to initialize the TDL wavenumber to that of an absorption line of a control gas after thermal cycling, step the TDL wavenumber in the presence of scan nonlinearities to the desired wavenumber which is assumed to be within a mode tuning range, lock to that desired wavenumber in spite of intermediate and long-term wavenumber drifts, and monitor continually the stability of the stable etalon vernier. The stepping and locking is accomplished using fm/harmonic detection of etalon fringes in quadrature in an auxiliary absorption spectrometer branch. This technique allows use of moderate finesse fringe patterns through its unique filtering capabilities and is insensitive to variations in TDL power. Details of the software and hardware design will be given including the design of the stable etalon.

We conclude that the characteristics of available laser diodes and aspects of their performance in closed-cycle cooler environments which may have made space flight systems impractical can be overcome through realizable control techniques.

## INTRODUCTION

In 1976, S.K. Poultney initiated a two-pronged research program to enable Perkin-Elmer to return to the flight spectroscopic sensor business. This program emphasized the FTS interferometer as a quantitative-survey instrument and the tunable laser spectrometer as a species-specific monitor. The tunable laser spectrometer was based on the Pb-salt tunable diode lasers. It encompassed the applications accessible to the Laser Heterodyne Spectrometer (LHS) and to the Tunable Diode Laser Absorption Spectrometer System (TDLSS). Following the assembly and testing of a CO<sub>2</sub>-laser based LHS, S.K. Poultney led the assembly and development of the state-of-the-art TDLSS for trace gas detection.

The following section describes the Perkin-Elmer TDLSS. The trace gas detection measurements with this system have been supported by the Federal Aviation Administration; first as a feasibility study (ref. 2) and more recently as a flight prototype activity led by M.D. Miller. These measurements with the TDLSS as well as many performance diagnostics supported by independent research programs have allowed us to obtain the measurements that we report in this paper. The goals of our investigations of the tunable laser spectrometer have been to determine those characteristics of the spectrometer which will limit its use for either of its two applications and to develop a potential solution for one of the most critical performance aspects. That aspect of performance is wavenumber purity and stability. Table I summarizes the wavenumber purity and stability required by the most demanding application; a laser heterodyne spectrometer measurement from space of reactive trace gases which cannot be contained in a reference cell and whose absorption lines have Doppler widths. The next two sections report the results of our wavenumber purity and stability diagnostics for performance characteristics inherent to tunable diode lasers and their environment, respectively. The final section describes a new concept for automatic wavenumber control which has been developed on an independent research program, and briefly summarizes our design for the necessary stable Fabry-Perot interferometer. Methods for ensuring a single mode at the detector are not discussed.

#### DESCRIPTION OF THE TUNABLE DIODE LASER SPECTROMETRIC SYSTEM (TDLSS)

The tunable diode laser spectrometric system consists of a laser source, its control environment, a sample cell, a detector, connecting optics, and a data acquisition system as shown in figure 1. The laser must normally be kept at temperatures near 25 K with a precision of tenths of millidegrees. It is normally tuned in wavenumber by applying an incremental drive current to the necessary bias current from a control module. This particular system possesses a digital control box which steps the drive current in small steps and synchronously clocks the A/D converter in the data acquisition system. This TDLSS can be operated in either the conventional am detection mode using the chopper or the fm/harmonic mode using one or more fm modulations superposed on the drive current. The signal out of the detector is appropriately demodulated and filtered before being digitized. A number of auxiliary optical devices are needed to control the laser output and to calibrate the laser wavenumber. These devices include a mode selector, a coarse wavenumber locator, calibration gas cells, calibration etalons, feedback isolators, etc. For use as a laboratory spectroscopy system, the TDLSS requires all these components as well as an executive software program.

The tunable laser source is a semiconductor diode of the Pb-salt family which can emit substantial amounts of power in a narrow spectral range in the midinfrared under the proper conditions. All of the lasers that we have used have been purchased from one commercial source, Laser Analytics, Inc. These diodes have yielded about 100 microwatts in each of several modes in the wavenumber region specified. Their lifetimes have been excellent (e.g. many months). Our specified wavenumbers have been reached within the available ranges of closed-cycle cooler temperatures and control-module bias and drive currents.

The TDL's must be operated under the proper temperature, mechanical-mount, and current conditions to insure best performance. For the laboratory TDLSS we selected an AIRCO closed-cycle cooler to provide the necessary cryogenic environment. In this environment, the TDL can operate between about 20 K and 50 K depending on its composition and the wavenumber desired. Temperature control and vibration mounting of the TDL was engineered by Perkin-Elmer and is described by Steinberg (ref. 1).

The TDL requires a current bias of up to 2 A in order to emit light. It is normally tuned in wavenumber by applying a variable drive current. Typical current tuning coefficients are  $0.011 \text{ cm}^{-1}/\text{mA}$ . We selected the analog current-control module made by Laser Analytics Inc. for the Laboratory TDLSS. We have found this to be a well-engineered unit. We have also found it convenient to supplement the analog current-control module with a digital control box. This digital control box steps the drive current in small steps and synchronously clocks both a chart recorder and the A/D converter in the data acquisition system. The data acquisition system records the digitized TDLSS scans for later analysis on the Perkin-Elmer time-sharing computer. The digital control box can scan at different rates and different tuning ranges, can scan down, can digitally set the bias current, and can accept either wavenumber control signals or several TDL modulation signals at an external summing junction.

This TDLSS can be operated in either of two detection modes: am chopping or fm/harmonic detection. The conventional am mode uses the chopper to modulate the light beam and the synchronous amplifier to demodulate and filter the detector signal. We use this mode for spectroscopic measurements of line positions, strengths, and widths (ref. 3). The fm/harmonic mode uses one or more fm modulations superposed on the TDL drive current and the synchronous amplifier to demodulate and filter the detector signal. We use this mode for trace gas detection because of its advantages for this application as discussed by Poultney et al. (ref. 2).

The detector is a broad response HgCdTe detector from Hughes/SBRC. It was purchased in conjunction with a matched, low noise preamplifier. The detector has performed well, but it was not specifically matched for any single application. Neither the field of view, the size, nor a cold filter has been selected to provide the lowest noise achievable in the present TDLSS.

The TDLSS optics consist entirely of offaxis parabolas and plano mirrors in order to minimize parasitic etalon noise and to make alignment straightforward. The optics are modular in form to allow convenient change of functions.

A number of auxiliary optical devices are needed to control the laser output and to calibrate the laser wavenumber. A grating monochromator (1/2 m Jarrell-Asch) has been used to locate the laser wavenumber (to about  $0.5 \text{ cm}^{-1}$ ), to study the axial mode structure of the TDL, and to select a single mode for transmission through the TDLSS. The monochromator has worked well in a laboratory environment and is essential for the TDL diagnostics and coarse wavenumber adjustment. The absolute wavenumber is best determined by the use of a gas with known absorption lines in a calibration cell.

For use as a laboratory spectroscopy system, the TDLSS requires an executive spectroscopy program which can read the digital records, normalize and calibrate each record, connect each short record (e.g.  $1 \text{ cm}^{-1}$ ) into the more normal spectroscopic display, print out the spectroscopic display, utilize analysis subprograms for the analysis of the data, and archive the data and results of the analysis. The flow chart of that executive spectroscopy program is shown in figure 2. Some of the analysis programs are library programs while others have been specifically written to accomplish nonlinear, least square fitting of spectral lineshapes (ref. 4).

## DIAGNOSTICS OF INHERENT TDL CHARACTERISTICS

### Capability to be Tuned to Desired Wavenumber

Our initial work with the NO TDL showed that we could not obtain an operating point which gave an output at the R(4.5) NO lines, but could obtain a good output at the nearby R(5.5) NO lines. This wavenumber search is executed by making a series of changes in both TDL heat sink temperature and drive current. The drive current tunes the TDL through joule heating in a finer degree than the temperature controller. The reason that some wavenumbers cannot be reached is related to the nature of the TDL output. This output consists of a number of modes with a fairly regular spacing and with varying amplitudes.

The number of modes is determined by the extent of the TDL gain curve. As the TDL temperature is tuned, these modes tune as much as a mode spacing, at which point the TDL cavity energy is sent into another mode. Certain operating points can be found where no modes are operating or where several modes are competing for the energy in an unstable fashion.

Once found, the operating points are a good guide as to how to obtain light at the desired wavenumbers during the same thermal cycle. These operating points do change with time and thermal cycling so that they may have to be optimized each time the TDL is used. The NO R(4.5) lines were accessible after the second thermal cycling, but the setting of the operating point was often tedious. A scan of these lines is shown in figure 3.

### Operating Point History

The operating point history of available TDL's is important because it will allow us to plan those field deployment techniques which will make possible the easy transfer of a characterized TDL to a field TDLSS or the quick recovery of a specified wavenumber after a thermal cycling in the field. We discuss in some detail the history of the NO TDL. This TDL has been in use since March 1979 and has been kept cold continuously except for 5 thermal cycles. Most of these cycles were caused by power outages. We find in general that the operating point changes such that the heat sink temperature must be decreased and the drive current increased as a function of time to achieve the same wavenumber as before. The location of this wavenumber is taken to be the peak of the room water-vapor line at  $1897.52 \text{ cm}^{-1}$ . Figure 4 presents the history of this operating point. We found it convenient to present this data as a graph of how the TDL wavenumber would have changed if the operating point had not been changed. In order to calculate this hypothetical performance, it was necessary to determine the thermal and current tuning rates of this TDL.

The TDL current tuning rate was measured by scanning through the well known R(5.5) NO lines at  $1897 \text{ cm}^{-1}$ . The current tuning rate was  $0.011 \text{ cm}^{-1}/\text{mA}$ . The thermal tuning rate was calculated from the operating point data of figure 4 for the dates between 8/23 and 9/19. Since the same absorption line was used each time, the temperature changes must correspond to the current changes. Use of the current tuning rate leads to a thermal tuning rate of  $1.2 \text{ cm}^{-1}/\text{K}$ . The hypothetical performance of the TDL wavenumber was then calculated relative to the operating point x on 3/29, using these rates and the actual operating point changes for each date. This performance is shown in figure 4. Most of the changes were small, which indicated that the same mode was used for all measurements. This observation means that one could

recover operation on a given line by a simple tuning of the drive current. Changes during a cycle are typically less than  $0.1 \text{ cm}^{-1}$ . The large change in wavenumber after cycle 2 is probably an indication that the TDL characteristics change so as to modify drastically the mode structure. The magnitude of the change is probably about equal to the mode spacing in this particular TDL. In fact, after this thermal cycle, the TDL could be tuned so as to allow the measurements of both the R(5.5) and R(4.5) NO line transitions.

It may also be helpful for field deployment considerations to summarize the operating point optimization process after a thermal change. Figure 5 shows a composite view of this process after the second thermal cycle. Figure 5(a) notes the TDL output before cycling as measured by the grating spectrometer superposed on a TDLSS trace of the ambient water vapor lines. Figure 5(b) shows the grating spectrometer trace of the TDL output after the cycle at the same heat sink temperature, but at a drive current which places the output at the previous wavenumber. Figure 5(c) shows the grating spectrometer trace of the TDL output after both temperature and current have been optimized to give near single mode performance at the previous wavenumber. Optimization of the operating point after a thermal cycle may thus require optimization of the mode structure as well.

#### Wavenumber Nonlinearity of the TDL

The fine wavenumber tuning of the TDL is accomplished by the joule heating of the drive current. For small drive currents compared to the TDL bias current, the wavenumber tuning is nearly linear with drive current. Scans like figure 3 in general possess a nonlinear current drive axis which must be calibrated for accurate work. One cannot simply interpolate between NO lines to locate the  $\text{N}_2\text{O}$  line, for example, to the precision required (e.g.  $10^{-4} \text{ cm}^{-1}$ ). The current drive axis is commonly calibrated through use of a scan of a stable etalon as shown in figures 6 and 7. The stable etalon used was a temperature stabilized Ge etalon commercially purchased with a finesse of 3 and a free spectral range of  $0.048 \text{ cm}^{-1}$  in the  $1897 \text{ cm}^{-1}$  region. Etalon fringe peaks are thus known to be equally spaced in the wavenumber domain.

One can expect a 5% nonlinearity over a  $1 \text{ cm}^{-1}$  tuning interval for 100 mA drive and 1 A bias.

We have studied the scan nonlinearities for a variety of purposes using our digital control and data acquisition system. Figure 6 shows an early scan of an etalon fringe pattern where the drive current at

each fringe peak has been recorded. The peak spacing in current steps and the tuning rate near each peak are listed in table II. This listing shows that the spacing increases as the drive current increases while the tuning rate decreases. These results are consistent with the joule heating picture. Figure 7 shows a digital record of a fringe scan overlaying the room water-vapor lines. We have analyzed this digital record with our etalon calibration software indicated in figure 2 and as outlined in table III. This more general analysis indicates that the tuning nonlinearity is more complicated than the quadratic expectation. We are continuing our analysis of the nonlinearities by trying to fit every point of the etalon curve rather than just the peak values.

### Axial Mode Structure

Axial mode structure is important to the performance of a TDLSS for at least three reasons. First, the presence of several modes at the same operating point requires in general the use of a grating monochromator (or other mode selector) to select the desired mode. The use of a grating spectrometer serves to increase the complexity of the TDLSS, introduce transmission loss, and introduce optical noise, although it is convenient for making coarse wavenumber identifications. Second, the mode structure may be such that the mode selector may not be able to reject very near or very far modes. Third, the selected mode may have fine wavelength structure which can only be diagnosed by other techniques. The latter two situations would serve to diminish the specificity of the TDLSS.

We present here some representative results of spectral scans of the TDL output which are relevant to field deployment. Figure 8 shows a TDL mode scan which indicates the very wide range ( $\sim 38 \text{ cm}^{-1}$ ) over which a mode selector may have to operate. Most TDL emission ranges span only about 10 to 15  $\text{cm}^{-1}$ . Figure 9 shows a mode scan which indicates the closest spacing of modes that may occur (i.e. about 2.2  $\text{cm}^{-1}$ ). Potential modes are actually spaced by 1.1  $\text{cm}^{-1}$  in this TDL, but operation at lower bias currents causes every other mode to drop out. At certain operating points, the selected single mode has fine structure. This fine structure has been studied in several ways, including heterodyne measurements with a local oscillator, calibration etalon scans, and scans of gas lines. In figure 10, we show examples of such scans of the NO doublet. The scan here happens to be the fm/second harmonic transform of the familiar NO doublet of  $R_{11}(5.5)$ . Figure 10(a) illustrates the mode structure (lower trace) and the absorption line scan (upper trace) when a single axial mode has been selected by the monochromator and when fine structure is not present. Figure 10(b) illustrates absorption line scans when the selected mode has fine structure. Each trace is taken with a different operating temperature and shows different fine structure. A typical spacing is 0.075  $\text{cm}^{-1}$  or 2.25 GHz. Heterodyne measurements with a 10 micron TDL indicated



fine structure with separations of 250 MHz. (See figure 11). Scans of a stable etalon also provide information on the fine structure of TDL axial mode from the discontinuity of the fringe pattern. Figure 12 shows a scan of a solid Ge etalon with a finesse of 3 and a free spectral range of  $0.047 \text{ cm}^{-1}$  using a  $940 \text{ cm}^{-1}$  TDL. At the left, the trace has the expected amplitude and shape. However, in the center a discontinuity appears and the amplitude of modulation drops sharply. This suggests the TDL sends out several closely spaced modes at this point.

Figure 5a and figure 5c show typical monochromator scans of TDL output after operating point optimization. For a common slit setting (i.e.  $0.27 \text{ mm}$  or  $1.6 \text{ cm}^{-1}$ ), we typically see about 5% of the TDL output in other distant modes. True single mode behavior to the 0.1% level was very seldom observed, as was the mode fine structure described above. Powers up to  $20 \mu\text{W}$  were delivered to the detector in a single mode selected by the monochromator of 25% transmission.

#### DIAGNOSTICS OF TDLSS CHARACTERISTICS DUE TO TDL ENVIRONMENT

The characteristics due to TDL environment included short-term wavenumber stability, the instrument lineshape function, and intermediate-term wavenumber stability. The short-term wavenumber stability was measured by using the heterodyne technique which was described by G. Steinberg (ref. 1). This study was carried out using a TDL chosen to overlap the available  $\text{CO}_2$ -laser lines near 10.6 microns. Figure 13 shows the heterodyne spectrometer and figure 14 shows the results achieved. The two lower traces indicate that the lineshape of the TDLSS is about 10 MHz in half-width (i.e.  $\sim 3 \times 10^{-4} \text{ cm}^{-1}$ ) for averaging times up to several minutes. Single traces at the top left show that the central wavenumber remains constant to about 2 MHz. Single traces at the top right indicate that the wings of the lineshape are due to large wavenumber excursions caused by the residual vibrations from the closed-cycle cooler. These residual vibrations could not be eliminated. The goal of resolving Doppler lines was, however, substantially met. The lineshape study of Doppler and Voigt lines reported by Poultney et al. (ref. 3) confirmed the heterodyne measurements of instrumental lineshape. Figure 15 is the measured shape of a  $\text{NH}_3$  line under Doppler conditions. The curve which connects the data points is the best fit Gaussian profile, with an instrument linewidth of  $4 \times 10^{-4} \text{ cm}^{-1}$ . The fitting procedure is described by Noll and Pires (ref. 4).

Intermediate-term wavenumber stability was estimated by using the TDLSS near 5.3 microns which was tuned to the half-width position

of NO  $R_{11}(5.5)$ , where the slope is the greatest. A sample cell of the spectrometer was filled with 0.9 Torr of NO, a pressure low enough for the absorption line to be Doppler limited, with a half-width at half maximum of about  $0.002 \text{ cm}^{-1}$ . The vertical deflection of the recorder pen then corresponds approximately to  $0.004 \text{ cm}^{-1}$ , or FWHM of the line. The diode current was then adjusted so that the diode wavelength was halfway down the absorption line; the point of maximum sensitivity to wavelength changes. Two traces are shown in figure 16. The upper trace shows the intermediate-term stability was about  $0.001 \text{ cm}^{-1}$ , with TDL temperature controller gain 50, while the short-term noise was much smaller. The intermediate fluctuation had a period of about 3 minutes. The short-term noise was larger ( $\sim 0.0008 \text{ cm}^{-1}$ ), but the intermediate-term noise was smaller, with the TDL temperature controller gain 100.

### WAVENUMBER CONTROL TECHNIQUE

The use of tunable diode lasers for laser heterodyne spectrometry requires that the issue of wavenumber control be addressed. There are various techniques to counteract the effects of thermal drift and thermal cycling of the laser. One of the most promising methods, based on counting and interpolating fringes of a stable Fabry-Perot interferometer, is described here.

The requirements for TDL wavenumber control imposed by spectroscopic and mission considerations have been summarized in table I. When the laser is turned on remotely, it must be tuned to the desired wavenumber even though its initial wavenumber may be uncertain due to thermal cycling. The tuning accuracy must be  $\pm 10^{-4} \text{ cm}^{-1}$  to ensure operation at the center of a Doppler-broadened line. Ideally, a cell containing the gas to be detected would be available at all times to provide a reference absorption line at precisely the correct wavenumber. However, in many cases it is not possible to carry a sample of a particular species with a flight spectrometer. Such tuning accuracy is useful only if the technique can also reduce the intermediate- and long-term drift of the laser to less than  $10^{-4} \text{ cm}^{-1}$ .

Our concept for wavenumber control is depicted with the aid of figure 17. First the TDL wavenumber is swept across its tuning range until an absorption line in a reference gas cell is found. We assume that the TDL wavenumber remains within a mode tuning range of the reference line during thermal cycling and operation. The reference line need only be as close as 1 or  $2 \text{ cm}^{-1}$  to the desired line position. Then the TDL mode structure is optimized for operation in this spectral region. The TDL is locked to the gas reference line and the position (in wavenumber space) of its output with respect to the etalon transmission curve is recorded. Next the TDL is tuned across a predetermined number of Fabry-Perot interferometer transmission peaks to the wavenumber

of the spectral line of interest. Finally the TDL is stabilized at that wavenumber by monitoring transmission through the etalon, and long-term drift of the etalon is compensated by a separate control system.

Detection of reference gas absorption and interferometer fringes is accomplished by modulation of the TDL at a frequency  $f_1$ , and modulation index  $A_1$ . As shown in figure 18, the first and second fm/harmonic signals are available to identify the position in wavenumber space of the laser output. The precise location of the TDL wavenumber to within one hundredth of a free spectral range of the interferometer requires accurate interpolation between transmission peaks.

One simple, elegant method of interpolation uses information found in first and second fm/harmonic detection of the etalon transmission function (also known as the Airy function). For very low values of finesse the Airy function is nearly sinusoidal on top of a DC component, resulting in nearly sinusoidal fm/harmonics (see figure 19a). Since the first two fm/harmonics have a  $90^\circ$  relative phase difference, their ratio is approximately proportional to the tangent of a quantity which varies linearly with wavenumber  $\sigma$ , as shown in figure 19(b). Therefore, by computing  $\theta$ , the arctangent of the ratio of the two harmonics of the Airy function, one obtains the wavenumber difference between the TDL output and any point on the etalon transmission function, except for an ambiguity due to the periodicity of the fringes. This ambiguity is resolved by counting the number of periods traversed as the TDL is tuned away from the reference line. Variations in TDL power do not present a problem because the ratio of fm/harmonic signals is used.

Use of moderate finesse etalons may degrade linearity below acceptable levels. The nonlinearity in the relationship between  $\theta$  and  $\sigma$  is due to the deviation of the Airy function from a sinusoid. The nonlinearity can be reduced by judicious choice of the modulation index  $A_1$ . As shown in figure 20, fm/harmonic detection is equivalent to filtering by a Bessel function in Fourier space. Here we use results of our complete analysis of the operation of a wavelength modulated spectrometer (ref. 5). The Fourier transform of the Airy function is a series of impulses at  $0, 2L/c, 4L/c, \text{etc.}$ , of decreasing magnitude. The impulse at  $2L/c$  represents the sinusoidal component of interest here; the others cause the nonlinearity. Detection of the first fm/harmonic,  $H_1$ , results in filtering by  $J_1(A_1)$ ; detection of the second fm/harmonic,  $H_2$ , results in filtering by  $J_2(A_1)$ . Variation of  $A_1$  greatly affects linearity, as is apparent from figure 21a. When  $A_1$  is about 0.4 times the etalon free spectral range, a minimum in nonlinearity is achieved. This minimum is not sufficient to allow utilization of a moderate finesse etalon of practical length (e.g.  $0.01 \text{ cm}^{-1}$ ).

Further improvement can be obtained by adding a second modulation at frequency  $f_2$ , with modulation index  $A_2$ . As shown in figure 20, the second modulation has the effect of filtering by  $J_0(A_2)$ , provided

the detection bandwidth is smaller than  $|f_1 - f_2|$ . The value of  $A_2$  may be chosen to cancel the contribution of the delta function at  $4L/c$ , the major source of nonlinearity. The improvement in interpolation linearity is seen in figure 21b, for an  $A_2$  of 0.19 times the free spectral range. Less than 1% nonlinearity may be achieved with reasonable etalon plate reflectivities of about 30%.

Drift of the etalon transmission curve, e.g. due to thermal expansion, can seriously degrade the accuracy of this technique. With a second laser (TDL 2), the drift of the etalon can be monitored and taken into account. If TDL 2 is continuously locked to a reference gas absorption line, its transmission through the etalon can accurately measure etalon drift. Use of fm/harmonic quadrature detection of TDL-2 transmission makes the monitor signal independent of TDL-2 power. The two lasers can be isolated by having their beams counterpropagating and orthogonally polarized. The detected etalon drift can provide continuous updating of the tuning of TDL 1, or can merely signal the need to repeat the TDL 1 wavenumber acquisition process.

In conclusion, a wavenumber control technique capable of meeting the most stringent requirements of a tunable laser heterodyne spectrometer system has been described and analyzed. Straightforward signal analysis principles have been used to adapt the method to practically realizable hardware. The requisite accuracy and long-term stability can be achieved with this system as long as the vernier etalon is stable between updates. Interpolation to 1% of a  $0.01 \text{ cm}^{-1}$  period etalon achieves the  $10^{-4} \text{ cm}^{-1}$  goal. The control technique and algorithms are discussed in greater detail by Wu and Poultney (ref. 6).

#### STABLE WAVENUMBER CONTROL ETALON

Our experience with solid Ge calibration etalons and adjustable air-space Fabry-Perot interferometers has led us to design a special purpose, air-space interferometer for the wavenumber control etalon. Table IV lists the features of this control etalon.

An air space etalon eliminates the refractive index inhomogeneity associated with thick germanium or silicon etalons. In addition, the temperature dependence of the index of air can be eliminated by sealing the space, and a spacer can be chosen with a lower coefficient of thermal expansion than that of a solid etalon.

Our air space interferometer uses a 25-cm reflector spacing to achieve a  $0.02 \text{ cm}^{-1}$  free spectral range. Figure 22 shows a schematic of the interferometer. Fabricating a 50-cm spacer would yield  $0.01 \text{ cm}^{-1}$ , which is our goal. The spacer is a fused silica tube, which provides inherently low thermal expansion. For fused silica,  $\alpha = 5 \times 10^{-7}/^\circ\text{C}$ . Only the so-called zero-expansion glasses have lower values,

and they are high cost items not readily available in tube form. Fused silica provides stability of  $10^{-3} \text{ cm}^{-1}/^{\circ}\text{C}$ .

The 2" outer diameter was chosen to be compatible with stock flat reflectors. The reflecting surfaces are optically contacted to the tube ends, assuring a moderately rugged, permanently aligned interferometer. The use of uncoated reflectors allows broadband performance. Zinc selenide provides 17% reflectivity and visible transmission for ease of system alignment. Germanium would give twice the reflectivity at the expense of this last feature, but we have determined the higher finesse unnecessary.

The outer surfaces of the reflectors are wedged with respect to the inner surfaces, and deliberate skewing of the wedges in both plates prevents the formation of a second etalon cavity. AR coatings could be utilized on the outer surfaces if experiment proves them necessary, but at the sacrifice of broadband performance.

With five-millimeter tube walls, the clear aperture is forty millimeters. Tube flex negligibly distorts the low finesse, even if the mounting is simple.

The design of the stable Fabry-Perot interferometer is described in more detail by McNally and Poultney (ref. 7).

## CONCLUSIONS

We conclude that the characteristics of available laser diodes and aspects of their performance in closed-cycle cooler environments which may have made space flight systems impractical can be overcome through realizable control techniques. In particular, wavenumber purity and stability issues have been thoroughly diagnosed and a conceptual design has been developed for a wavenumber control system which can resolve performance questions related to these key issues.

## REFERENCES

1. Steinberg, G.N.: Wavenumber Stability of a Laser Diode Mounted in a Closed Cycle Helium Refrigerator. *Rev. Sci. Instrum.*, vol. 50, no. 12, Dec. 1979, pp. 1622-1625.
2. Poultney, S.; Steinberg, G.; Pires, A.; Miller, M.; Chen, D.; Macoy, N.; Noll, R.; and Grossman, W.: Tunable Diode Laser Absorption Spectrometer as the Stratospheric Measurement System for the High Altitude Pollution Program - A Feasibility Study. Perkin-Elmer Report No. 14752, The Perkin-Elmer Corporation, Danbury, CT., 1980.
3. Poultney, S.; Steinberg, G.; Noll, R.; Pires, A.; Chen, D.; and Miller, M.: The Position of Water Vapor Lines near 5 Microns, NH Line Shape Measurements, and Comments on Wavenumber Calibration using Tunable Diode Laser Spectrometer. Published in 34th Annual Symposium on Molecular Spectroscopy, Ohio State University, Columbus, Ohio, June 11-15, 1979.
4. Noll, R.; and Pires, A.: A New Nonlinear Least Square Algorithm for Voigt Spectral Lines. *Applied Spectroscopy*, vol. 34, no. 3, May 1980, pp. 351-360.
5. Pires, A.; Poultney, S.; Chen, D.; and Miller, M.: Theory and Practice of the Wavelength Modulated Spectrometer. Preliminary report published in Pittsburgh Conference on Analytical Chemistry and Applied Spectroscopy, Atlantic City, New Jersey, March 10-14, 1980.
6. Wu, F.; and Poultney, S.: Wavenumber Control Techniques for Tunable Diode Laser Spectrometer. Perkin-Elmer Report No. 14762, The Perkin-Elmer Corporation, Danbury, CT., 1980.
7. McNally, M.; and Poultney, S.: Design of a Stable Fabry-Perot Etalon for TDL Spectrometer Calibration and Control. Perkin-Elmer Report No. 14763, The Perkin-Elmer Corporation, Danbury, CT., 1980.

TABLE I.- REQUIREMENTS FOR TDL WAVENUMBER CONTROL

- o Following Turn-On, TDL must Automatically Tune to Desired Wavenumber
- o Tuning Accuracy must be better than  $\pm 10^{-4} \text{ cm}^{-1}$  (10% of Doppler Width), even if a reference cell with absorption line at desired wavenumber is not available
- o Short-term Drift must be less than  $10^{-4} \text{ cm}^{-1}$
- o Intermediate-Term Drift must be less than  $10^{-4} \text{ cm}^{-1}$
- o Long-term Drift must be less than  $10^{-4} \text{ cm}^{-1}$  for periods of hours
- o TDL Output at Detector must consist of Single Mode of Adequate Power

TABLE II.- PEAK SPACING IN CURRENT STEPS AND TUNING RATE  
NEAR EACH PEAK

Fringe	TDL Current (Amp)	$\Delta I$ (ma)	$\frac{\partial \sigma}{\partial I}$ (cm <sup>-1</sup> /ma)
1	1.7222	4.0 <u>0</u> +0.1	0.0120 = 0.0003
2	1.7262	3.9	0.0123
3	1.7301	3.9	0.0123
4	1.7340	4.1	0.0117
5	1.7381	3.9	0.0123
6	1.7420	4.1	0.0117
7	1.7461	4.1	0.0117
8	1.7502	4.2	0.0114
9	1.7544	4.2	0.0114
10	1.7586	4.2	0.0114
11	1.7628	4.2	0.0114
12	1.7670	4.3	0.0112
13	1.7713	4.3	0.0112
14	1.7756		



TABLE III.- PROCEDURE FOR WAVENUMBER SCALE CALIBRATION

1. Find Etalon Peak Locations

- o locate peak vicinity
- o quadratic fit fringe to locate fringe center

2. Expand peak positions in nth order polynomial

- o assign fringe number to peak
- o least-squares fit nth order polynomial

$$y = a_0 + a_1x + a_2x^2 + \dots$$

where  $x$  = fringe position

$y$  = fractional fringe number

3. Calibrate wavenumber scale using known FSR and reference line

- o  $\sigma(x) = \text{FSR} \cdot [a_0 + a_1x + a_2x^2 \dots] + \sigma_{\text{ref}}$

TABLE IV.- ETALON DESIGN FEATURES

- o Inherent Temperature Stability -  $10^{-3}$   $\text{cm}^{-1}/^{\circ}\text{C}$  with fused silica spacer
- o Short Free Spectral Range -  $0.02$   $\text{cm}^{-1}$  with 25 cm cavity
- o Permanent Alignment - Solid Assembly of Reflectors to Spacer
- o Simple System Insertion - Transparent in Visible for Alignment
- o Broadband Reflectivity - Available through Fresnel Reflection
- o Large Aperture - 40 mm C.A.
- o Freedom from Secondary Etalon Effects - Uses Wedged Reflectors
- o Freedom from Index Inhomogeneity - Assured by Closed Air-Space Design

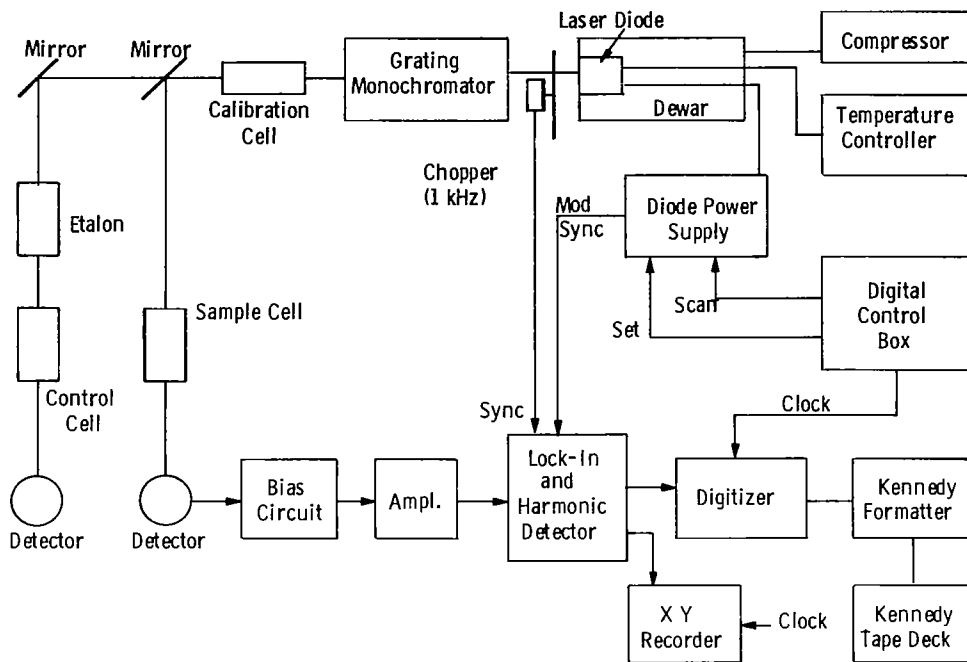


Figure 1.- Tunable diode laser absorption spectrometer; uses all reflective optics and can provide graphical or IBM-compatible digital records.

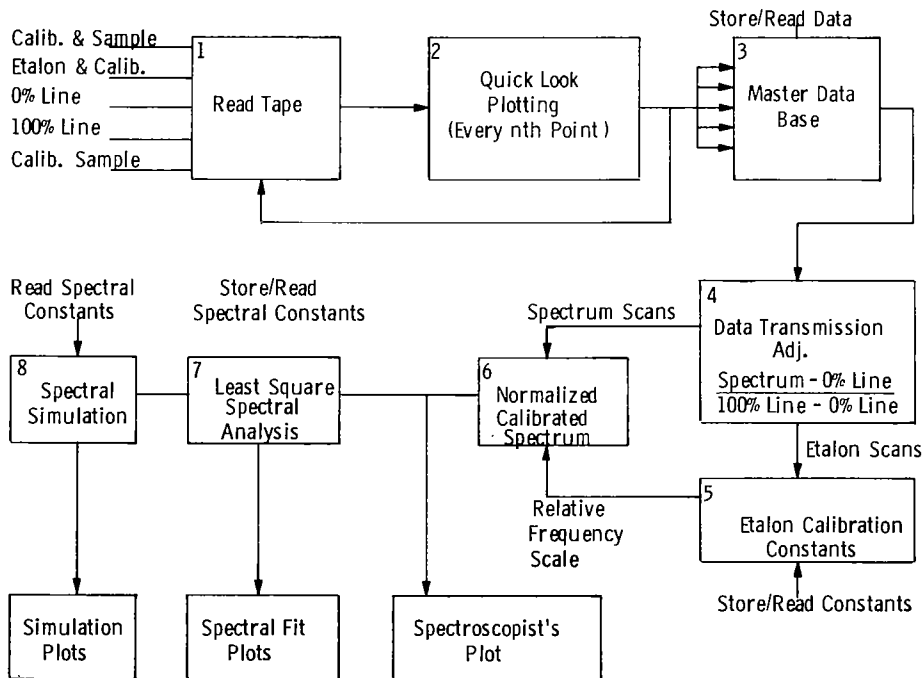


Figure 2.- Flowchart of executive spectroscopy software for tunable diode laser absorption spectrometer.

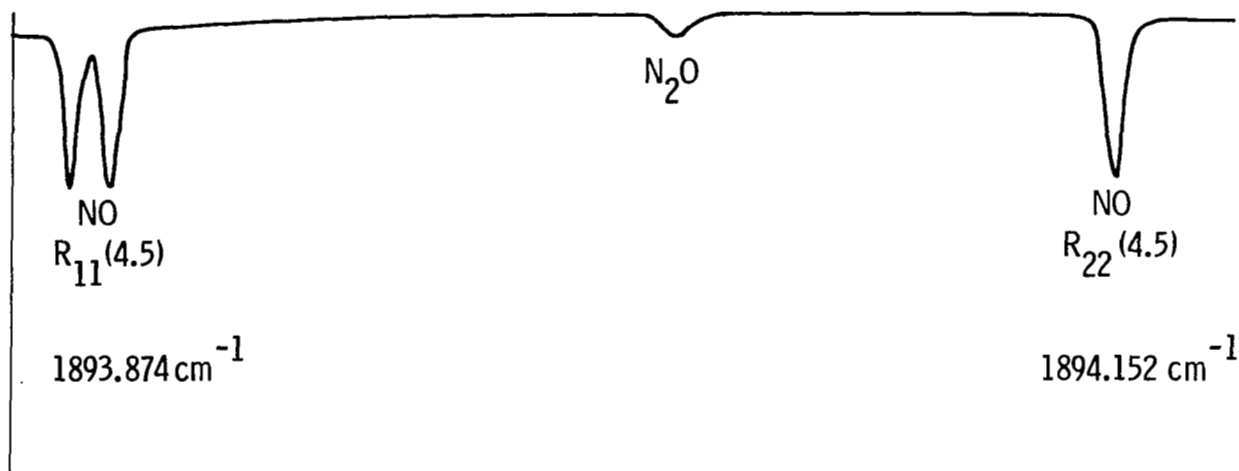


Figure 3.- Laboratory NO absorption spectrum for R(4.5) transition near 1894 cm<sup>-1</sup>. Also shown is weak N<sub>2</sub>O line due to 10 Torr N<sub>2</sub>O added to second sample cell.

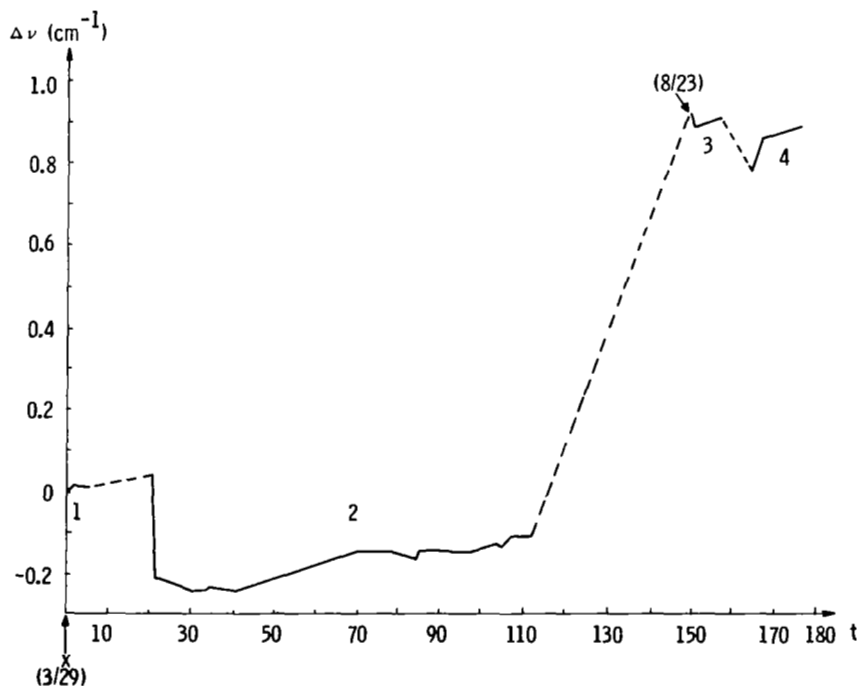


Figure 4.- TDL operating point history. During operation, operating point would change by about 0.1 cm<sup>-1</sup> over longer term, with even larger changes occurring during some thermal cycles.

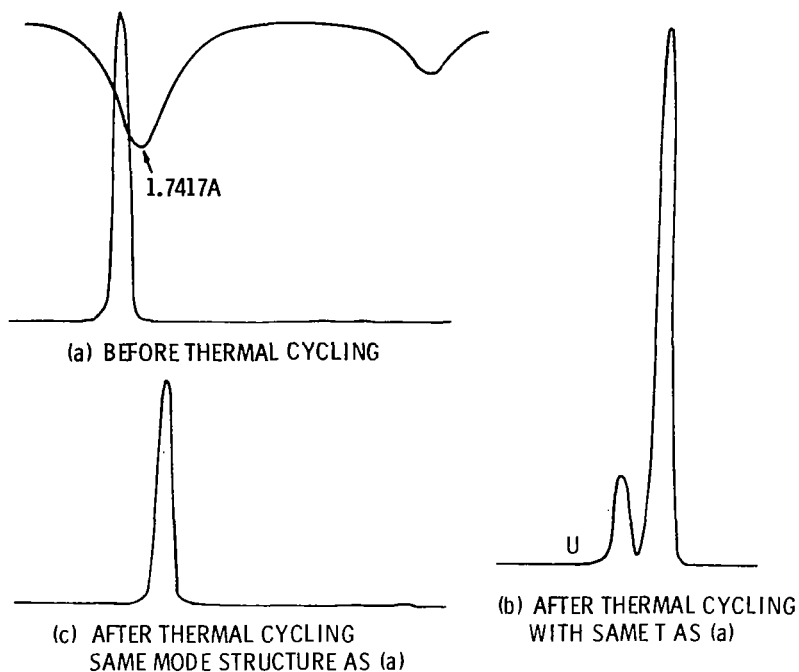


Figure 5.- Optimization of TDL mode structure after thermal cycling. After each thermal cycle, TDL operating point changes such that heat sink temperature must be decreased and drive current increased to achieve same wavenumber and to obtain as much power in single mode as possible.

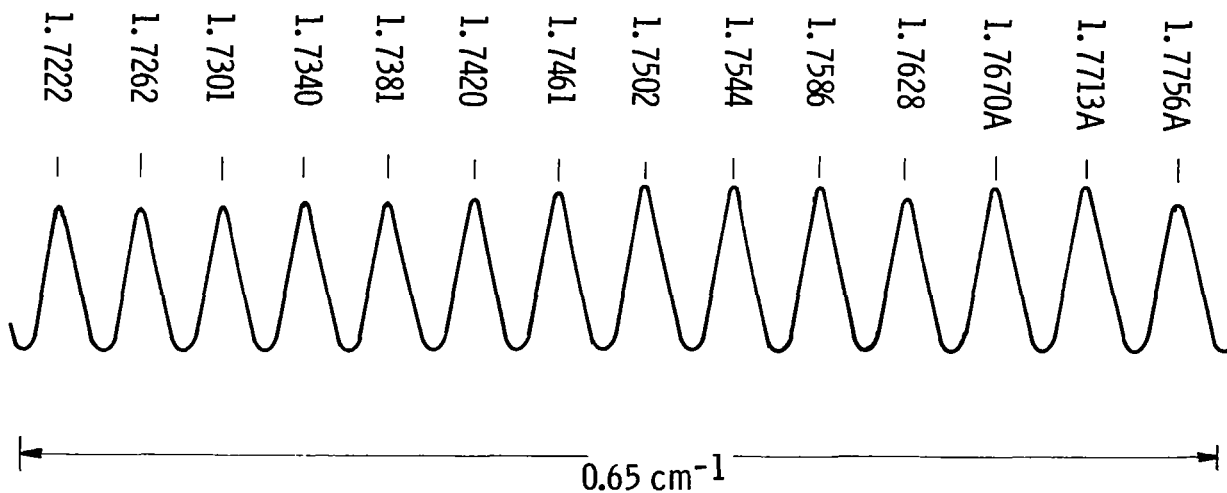


Figure 6.- Germanium etalon fringe scan. Drive current at each fringe peak is indicated. FSR of etalon is  $0.048 \text{ cm}^{-1}$ .

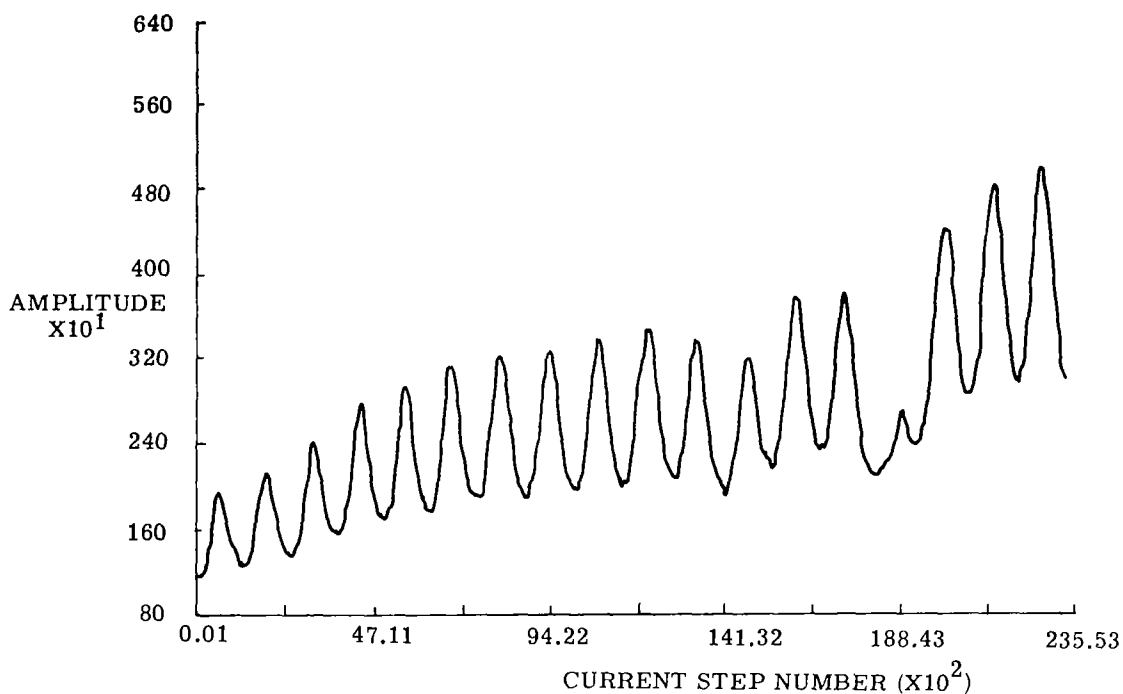


Figure 7.- Digitized etalon scan. Etalon fringes distorted by H<sub>2</sub>O lines are discarded from fitting process.

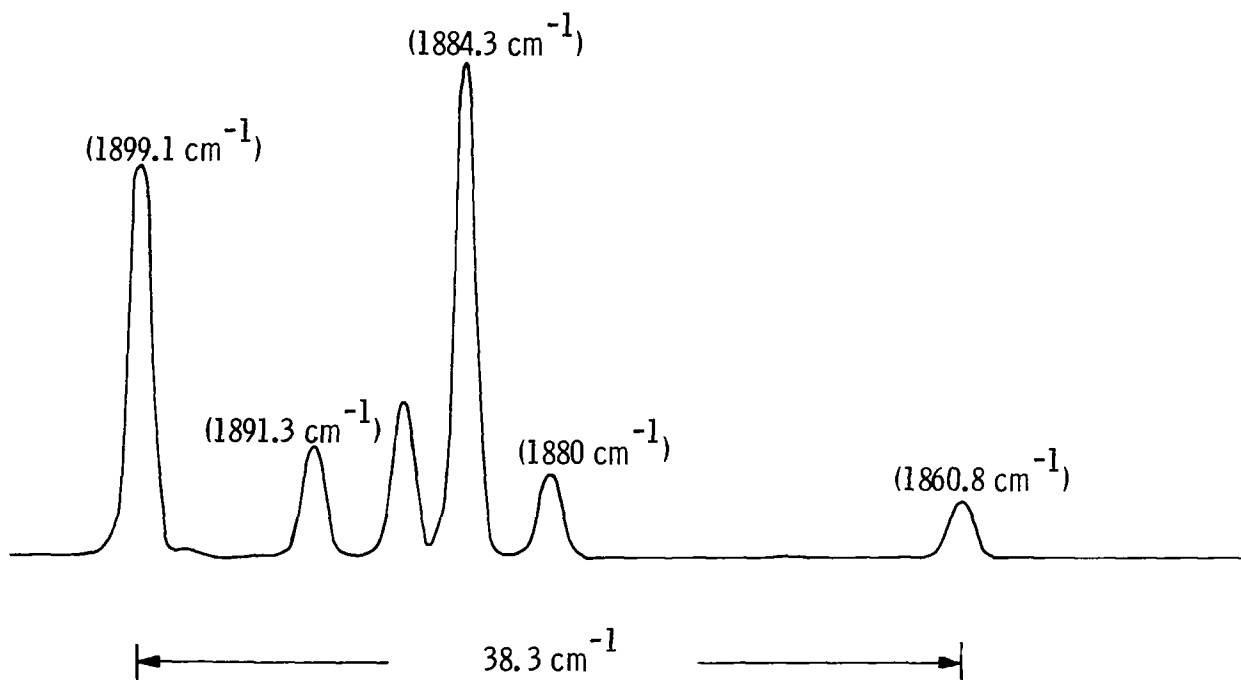


Figure 8.- TDL mode scan; indicates very wide range over which mode selector may have to operate.

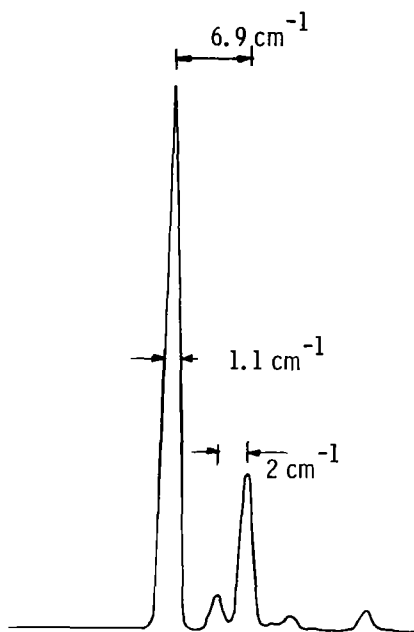
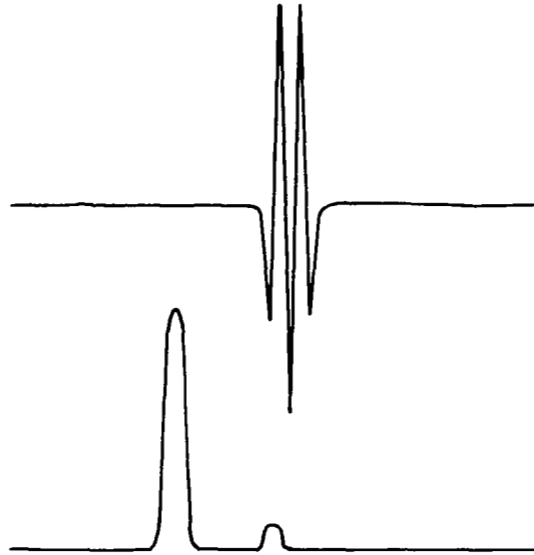
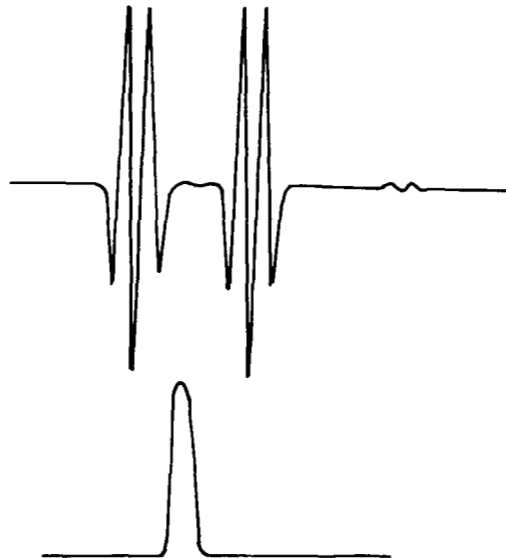


Figure 9.- TDL mode scan; indicates closest spacing of modes which may occur (i.e. about  $2 \text{ cm}^{-1}$ ).



(a) Single axial mode selected by monochromator when fine structure is not present.



(b) Absorption line scans when selected mode has fine structure.

Figure 10.- Absorption line scan evidence for fine mode structure, showing mode structure (lower trace) and absorption line scan (upper trace). Each trace is taken with different operating temperature and shows different fine structure. Typical spacing is  $0.075 \text{ cm}^{-1}$  or  $2.25 \text{ GHz}$ .



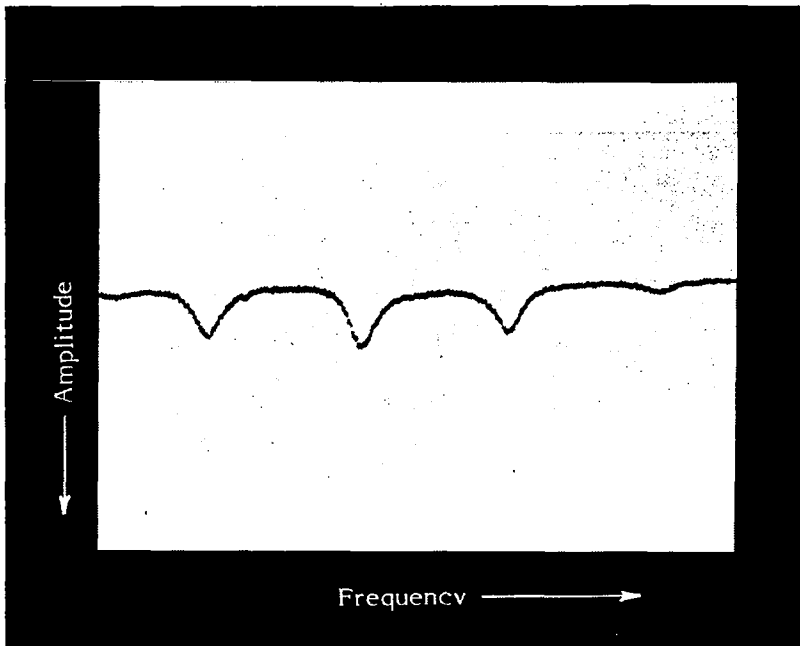


Figure 11.- Heterodyne beat between CO<sub>2</sub> laser and diode laser fixed near 10.6 micrometers showing fine structure of single axial mode. Peaks are separated by 250 MHz.

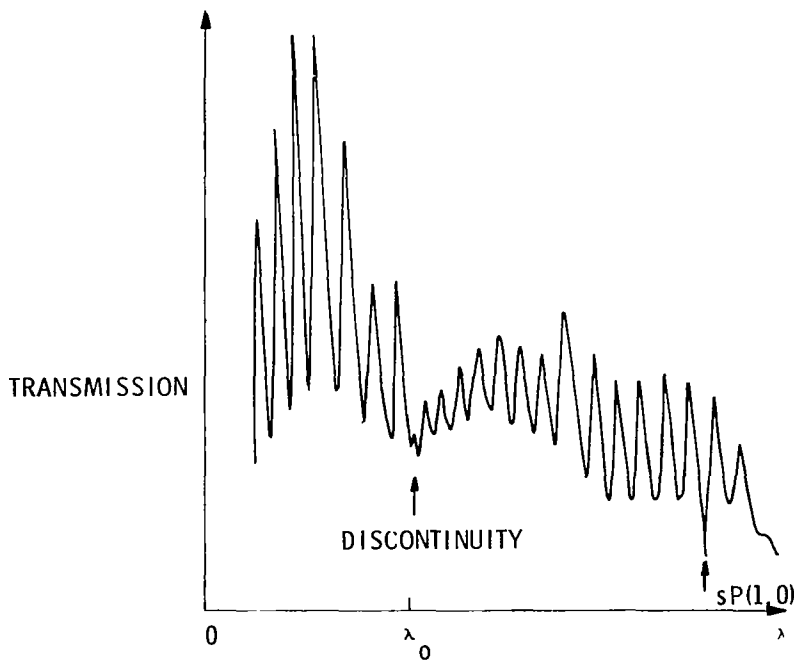


Figure 12.- Calibration etalon evidence for mode fine structure with 10.6 microns TDL. Note discontinuity at marked  $\lambda_0$ .

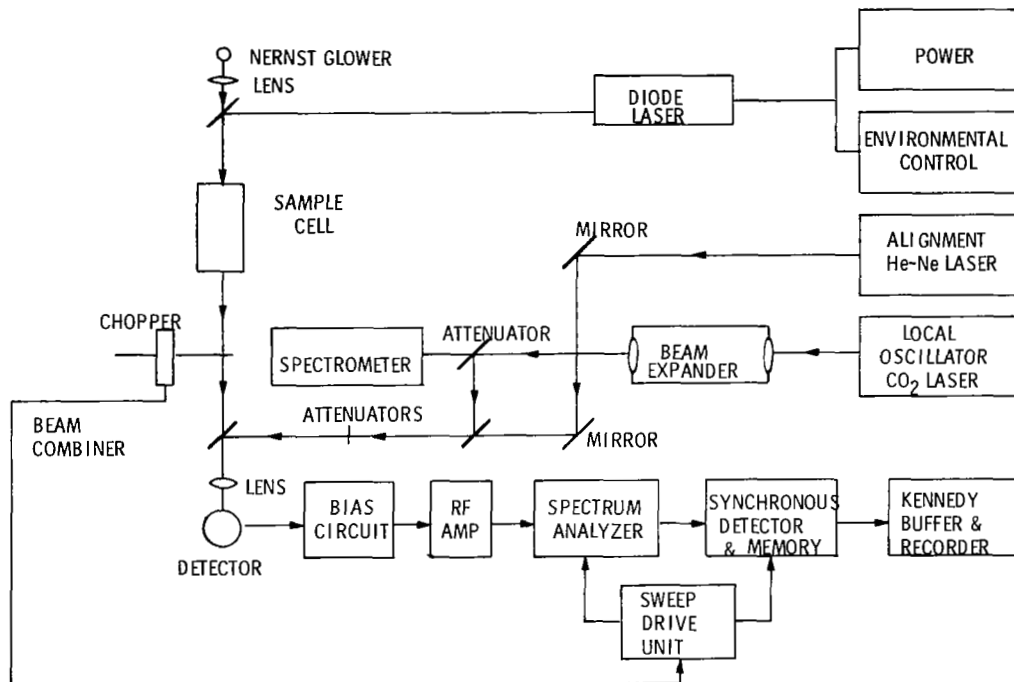


Figure 13.- Schematic diagram of heterodyne spectrometer with digital synchronous detector.

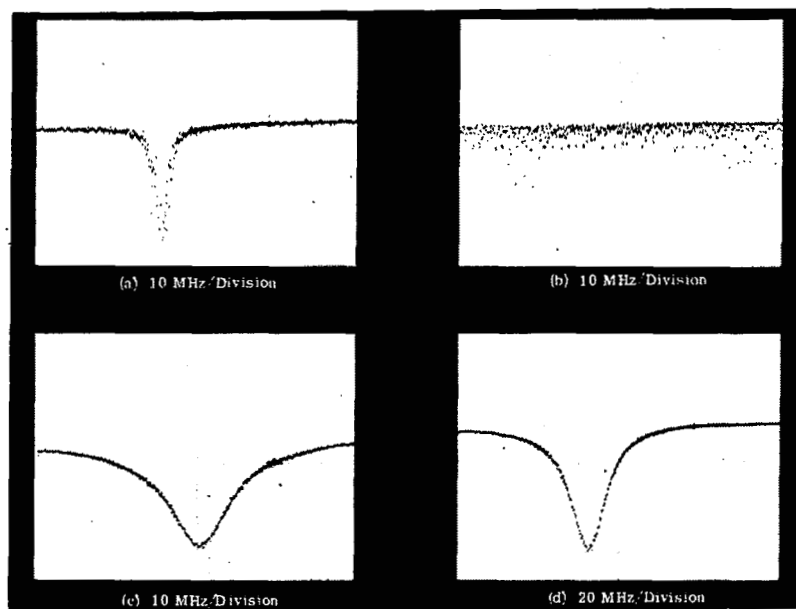


Figure 14.- Short-term stability of laser diode output wavelength. Results obtained with CO<sub>2</sub> laser heterodyne spectrometer for time period stated. All frequency sweeps are 10 MHz/div. except for (d) where it is 20 MHz/div. Equivalent line shape is shown to be 20 MHz FWHM in (c) and (d), for 75-s averaging time and is thought to be due to residual vibrations. Both (a) and (b) are selected single sweeps.

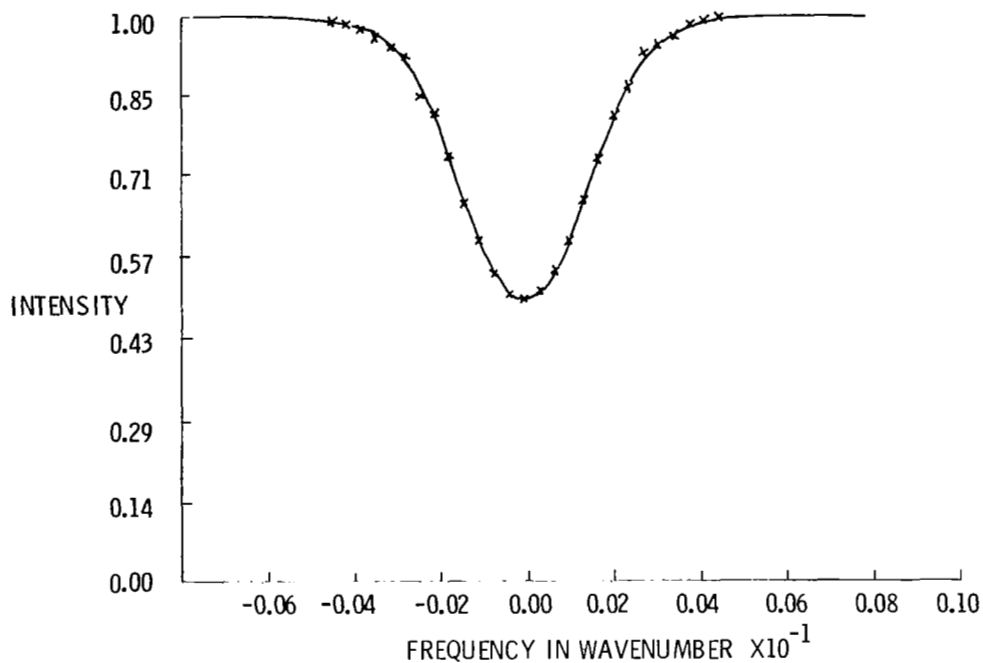


Figure 15.- Shape of  $sP(1,0)$  line of  $NH_3$  near  $948\text{ cm}^{-1}$  under Doppler conditions in 2.5-cm cell. Points indicate data. Curve is best fit using least-square technique.

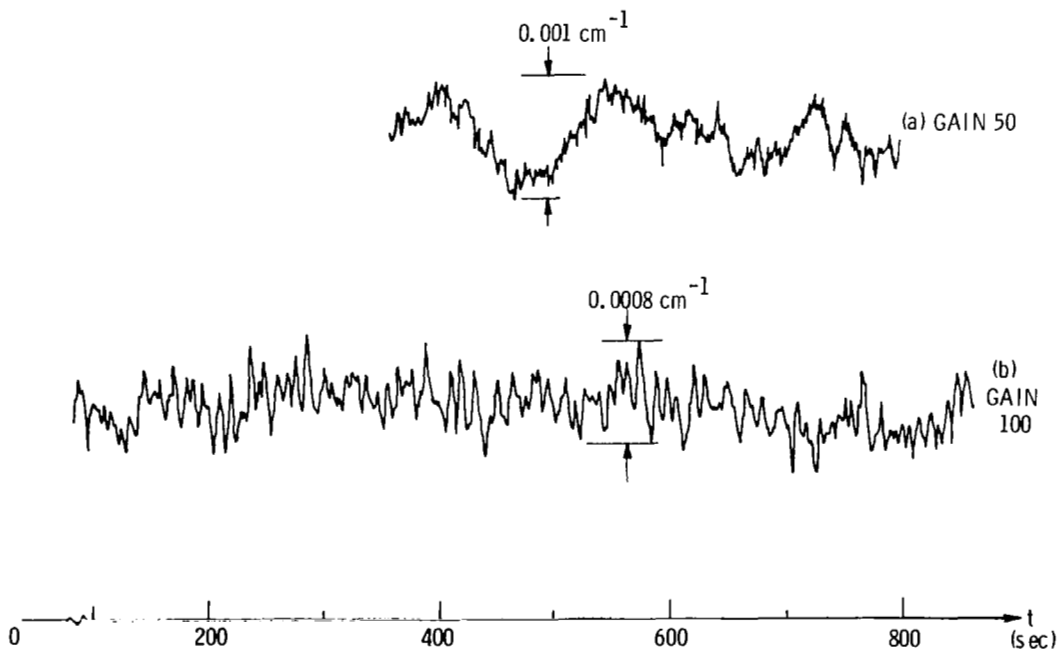


Figure 16.- Intermediate-term wavenumber stability; about  $0.001\text{ cm}^{-1}$  with TDL temperature controller gain 50 (upper trace). Lower trace shows stability  $0.0008\text{ cm}$  with TDL temperature controller gain 100.

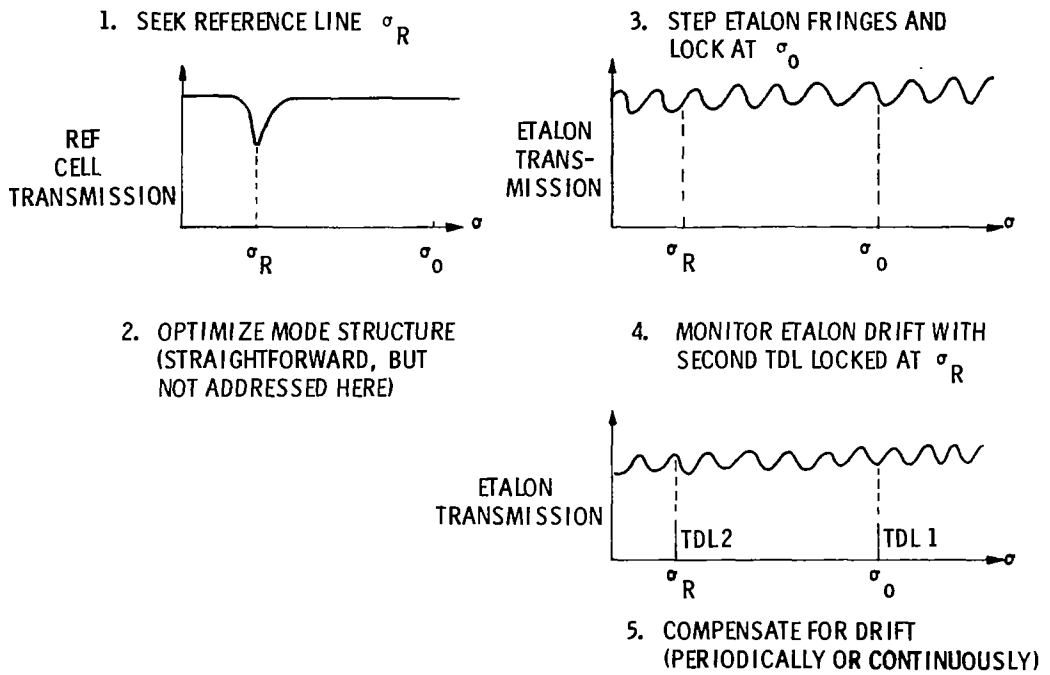


Figure 17.- Use of stable etalon for wavenumber control.  $\sigma_R$  is wavenumber of reference gas absorption line;  $\sigma_0$  is desired operating wavenumber.

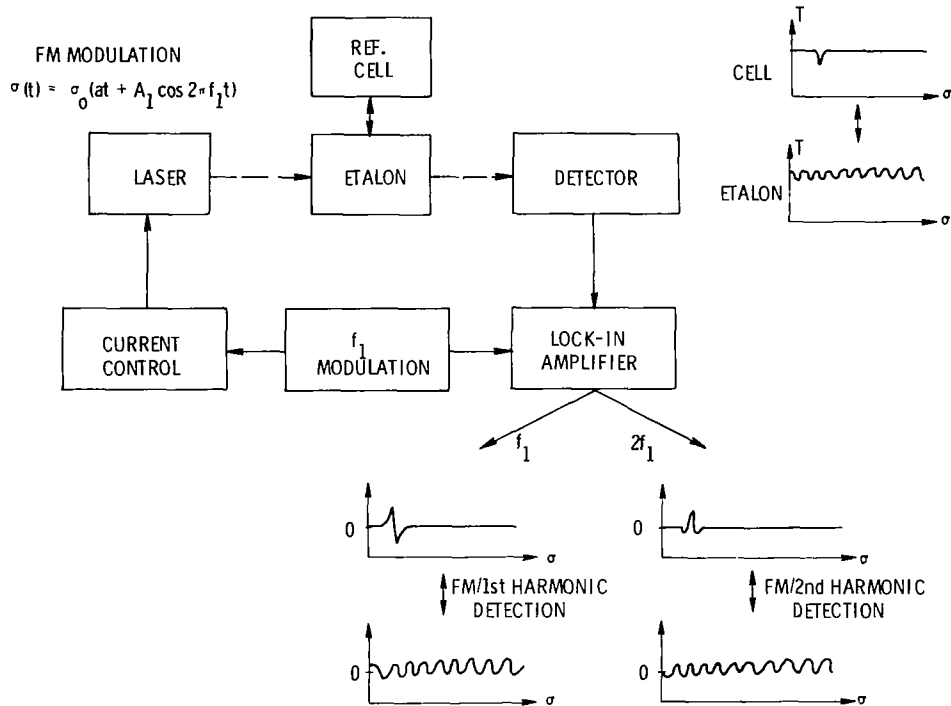
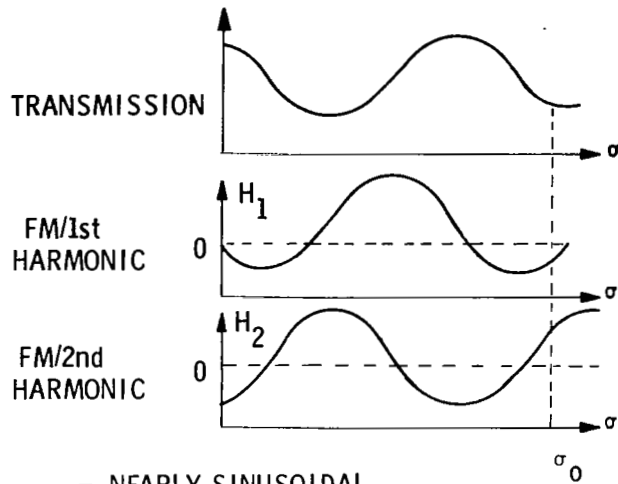
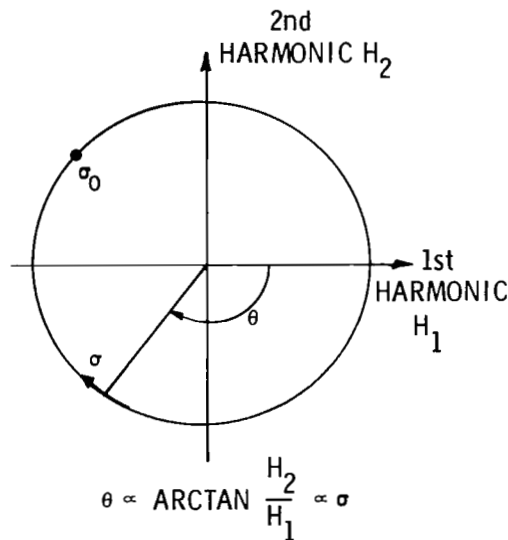


Figure 18.- Schematic of wavenumber control system. Transmission of reference cell is monitored until TDL is locked to reference line. Then etalon transmission is monitored for fringe position and stepping.



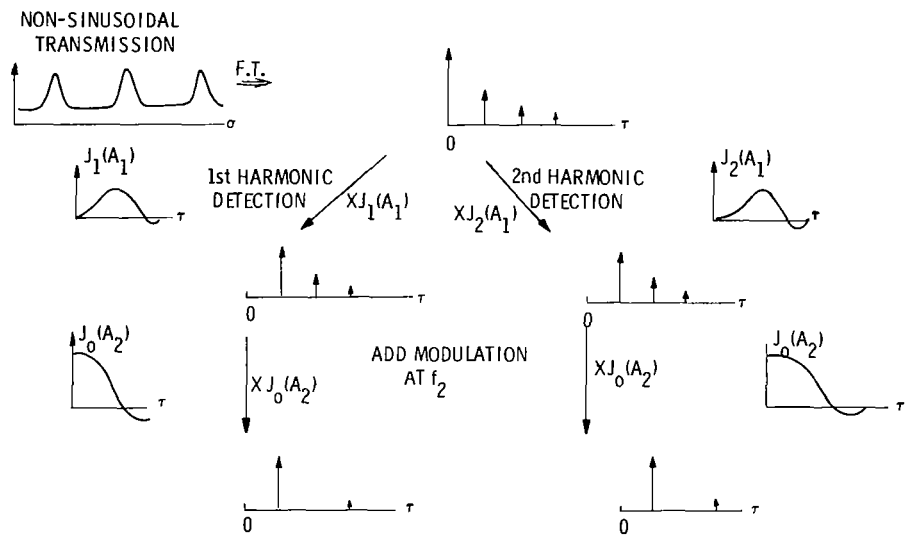
- NEARLY SINUSOIDAL
- 1st AND 2nd HARMONICS ARE  $\frac{\pi}{2}$  OUT OF PHASE
- $\theta$  IS INDEPENDENT OF TDL POWER

(a) Etalon transmission function and its fm/harmonic detection signals  $H_1$  and  $H_2$ .



(b) Relation between  $H_1$ ,  $H_2$ , and  $\theta$ , which is proportional to wavenumber (approximately). As laser is tuned,  $\theta$  increases linearly with wavenumber.

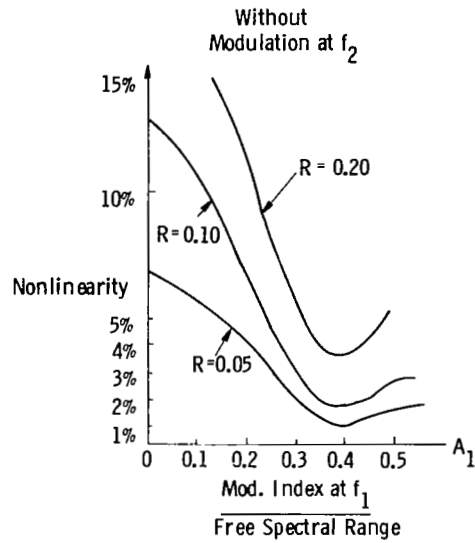
Figure 19.- Etalon fringe interpolation.



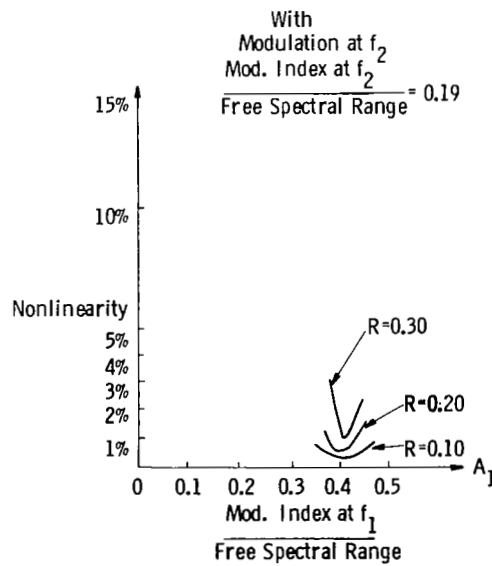
- NEARLY SINUSOIDAL FM/HARMONIC SIGNALS
- $\theta$  VERY LINEAR IN  $\sigma$
- PHASE SHIFT STILL  $\pi/2$

Figure 20.- Filtering by Bessel functions for improved linearity. TDL is modulated with modulation index  $A_1$  at frequency  $f_1$  and index  $A_2$  at  $f_2$ . Demodulation at first harmonic ( $f_1$ ) and second harmonic ( $2f_1$ ) corresponds to filtering by  $J_1(A_1)$  and  $J_2(A_1)$ , respectively, followed by  $J_0(A_2)$ .

$$\text{Nonlinearity} = \frac{\text{Max. Error of Linear Approximation}}{\text{Free Spectral Range}}$$

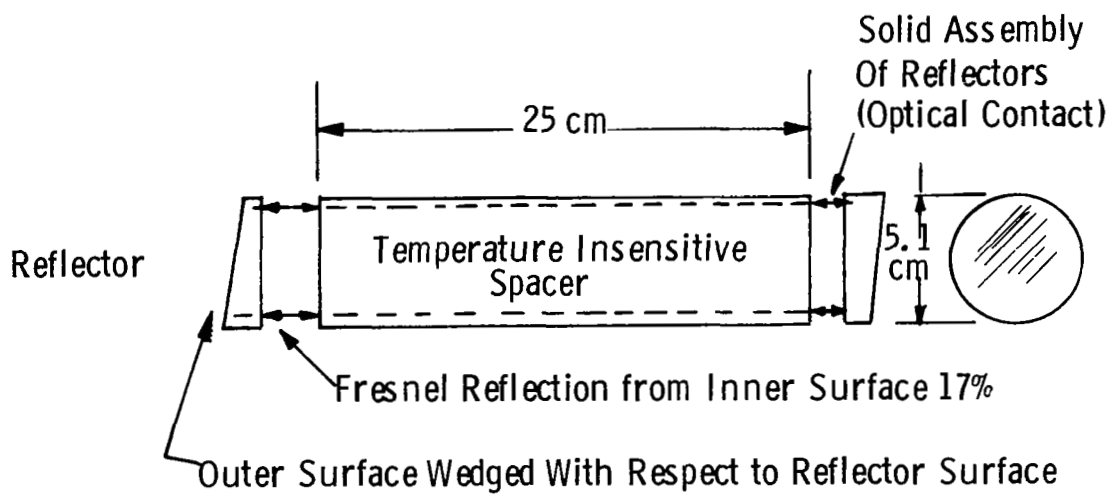


(a) Effect of modulation index  $A_1$  at frequency  $f_1$  on interpolation linearity.



(b) Same as (a), but with second modulation at  $f_2$ . Much better linearity can be achieved.

Figure 21.- Interpolation linearity.



Tube Flexing has Negligible Effect on Finesse - - Mounting is Non-critical

Figure 22.- Air space etalon; constructed of two zinc selenide flats, contacted to fused silica tube which acts as spacer. Fresnel reflection from inner surfaces of ZnSe plates is used, and outer surfaces are wedged to eliminate accidental etalon behavior.